Inorg. Chem. **2004**, *43*, 482–489

Photochromism of Metal Complexes Composed of Diarylethene Ligands and Zn(II), Mn(II), and Cu(II) Hexafluoroacetylacetonates

Kenji Matsuda,*,†,‡ Kohsuke Takayama,† and Masahiro Irie*,†

Department of Chemistry and Biochemistry, Graduate School of Engineering, Kyushu University, 6-10-1 Hakozaki, Higashi-ku, Fukuoka 812-8581, Japan, and PRESTO, JST, Japan

Received August 30, 2003

Metal complexes composed of bidentate 1,2-bis(2-methyl-5-(4-pyridyl)-3-thienyl)perfluorocyclopentene (**1a**) and monodentate 1-(2-methyl-5-phenyl-3-thienyl)-2-(2-methyl-5-(4-pyridyl)-3-thienyl)perfluorocyclopentene (**2a**) photochromic ligands and $M(hfac)_2$ (M = Zn(II), Mn(II), and Cu(II)) were prepared, and their photoinduced coordination structural changes were studied. X-ray crystallographic analyses showed the formation of coordination polymers and discrete 1:2 complexes for bidentate and monodentate ligands, respectively. The complexes underwent reversible photochromic reactions by alternate irradiation with UV and visible lights in solution as well as in the single-crystalline phase. Upon photoirradiation with UV and visible light, the ESR spectra of the copper complexes of **1a** reversibly changed. While the open-ring isomer gave an axial-type spectrum, the photogenerated closed-ring isomer showed a rhombic-type spectrum. This indicates that the photoisomerization induced the change in the coordination structure.

Introduction

Photochromic compounds have attracted remarkable attention because of their potential ability for optical memory media and optical switching devices.[1] Among them, diarylethenes with heterocyclic aryl groups are the most promising compounds for the applications because of their fatigue resistant and thermally irreversible photochromic properties.[2] Moreover, it has recently been found that some diarylperfluorocyclopentenes having thiophene or benzothiophene rings undergo photochromic reactions even in the single-crystalline phase.[3]

Diarylethenes have been proven as excellent photoswitching devices as well. The open- and closed-ring isomers of the diarylethenes differ from each other not only in their absorption spectra but also in various physical and chemical properties such as geometrical structures, refractive indices, dielectric constants, and oxidation/reduction potentials. These property changes have been utilized to control functions of photoresponsive molecules and polymers, such as host−guest interactions,[4] alignment of liquid crystals,[5] and electronic conductions.[6] One of the novel examples is the photoswitching of magnetic interactions.[7] When nitroxide radicals were located at both ends of the aryl groups of the diarylethenes, the magnetic interaction between nitroxide radicals can be changed more than 150-fold by photoirradiation. The

* To whom correspondence should be addressed. E-mail: kmatsuda@cstf.kyushu-u.ac.jp (K.M.); irie@cstf.kyushu-u.ac.jp (M.I.).

† Kyushu University.

‡ PRESTO, JST.

(1) (a) *Molecular Switches*; Feringa, B. L., Ed.; Wiley-VCH: Weinheim, 2001. (b) Brown, G. H. *Photochromism*; Wiley-Interscience: New York, 1971. (c) Dürr, H.; Bouas-Laurent, H. *Photochromism: Molecules and Systems*; Elsevier: Amsterdam, 2003.

(2) (a) Irie, M. *Chem. Rev.* **2000**, *100*, 1685−1716. (b) Irie, M.; Uchida, K. *Bull. Chem. Soc. Jpn.* **1998**, *71*, 985−996. (c) Irie, M.; Fukaminato, T.; Sasaki, T.; Tamai, N.; Kawai, T. *Nature*, **2002**, *420*, 759.

(3) (a) Irie, M.; Uchida, K.; Eriguchi, T.; Tsuzuki, H. *Chem. Lett.* **1995**, 899−900. (b) Kobatake, S.; Yamada, T.; Uchida, K.; Kato, N.; Irie, M. *J. Am. Chem. Soc.* **1999**, *121*, 2380−2386. (c) Kobatake, S.; Yamada, M.; Yamada, T.; Irie, M. *J. Am. Chem. Soc.* **1999**, *121*, 8450−8456. (d) Yamada, T.; Kobatake, S.; Irie, M. *J. Am. Chem. Soc.* **2000**, *122*, 1589−1592. (e) Irie, M.; Lifka, T.; Kobatake, S.; Kato, N. *J. Am. Chem. Soc.* **2000**, *122*, 4871−4876. (f) Kodani, T.; Matsuda, K.; Yamada, T.; Kobatake, S.; Irie, M. *J. Am. Chem. Soc.* **2000**, *122*, 9631−9637. (g) Yamada, T.; Kobatake, S.; Irie, M. *Bull. Chem. Soc. Jpn.* **2000**, *73*, 2179−2184. (h) Shibata, K.; Muto, K.; Kobatake, S.; Irie, M. *J. Phys. Chem. A* **2002**, *106*, 209−214. (i) Kobatake, S.; Uchida, K.; Tsuchida, E.; Irie, M. *J. Chem. Soc., Chem. Commun.* **2002**, 2804−2805.

(4) (a) Takeshita, M.; Uchida, K.; Irie, M. *J. Chem. Soc., Chem. Commun.* **1996**, 1807−1808. (b) Kawai, S. H. *Tetrahedron Lett.* **1998**, *39*, 4445−4448. (c) Takeshita, M.; Irie, M. *Tetrahedron Lett.* **1998**, *39*, 613−616. (d) Takeshita, M.; Irie, M. *J. Org. Chem.* **1998**, *63*, 6643−6649.

(5) (a) Denekamp, C.; Feringa, B. L. *Adv. Mater.* **1998**, *10*, 1080−1082. (b) Yamaguchi, T.; Inagawa, T.; Nakazumi, H.; Irie, S.; Irie, M. *Chem. Mater.* **2000**, *12*, 869−871. (c) Uchida, K.; Kawai, Y.; Shimizu, Y.; Vill, V.; Irie, M. *Chem. Lett.* **2000**, 654−655.

(6) (a) Gilat, S. L.; Kawai, S. H.; Lehn, J.-M. *J. Chem. Soc., Chem. Commun.* **1993**, 1439−1442. (b) Gilat, S. L.; Kawai, S. H.; Lehn, J.-M. *Chem. Eur. J.* **1995**, *1*, 275−284. (c) Kawai, T.; Kunitake, T.; Irie, M. *Chem. Lett.* **1999**, 905−906.

10.1021/ic035020r CCC: $27.50
Published on Web 12/18/2003

switching is due to the changes in π-conjugated chain length between the two isomers.

Coordination-driven self-assembly is an important strategy to construct supramolecular architecture.[8] Predesigned geometry of the metal core and organic ligands determines the final assembled structure, which can be two- or three-dimensional. An assembled structure can have unique physical properties, such as magnetism[9] or gas adsorption.[10] Precisely controlled magnetic exchange interactions between the metal centers in the complex afford many unique molecule-based magnetic materials. Highly porous robust metal-organic frameworks afford the ideal platform for the gas adsorption.

Although there are several reports on the synthesis of metal complexes of photochromic diarylethenes,[11] no report on the photoreactivity in the single-crystalline phase nor on the photoswitching of the coordination structure has been reported.[12] We have prepared complexes composed of monodentate or bidentate diarylethene pyridyl ligands and transition metals (Zn(II), Cu(II), and Mn(II)) and examined the reactivity in solution as well as in the crystalline phase. When the photochromic reaction takes place efficiently, the physical properties of the metal complexes are expected to be reversibly changed. To prove the photoswitch, the coordination structural change with photochromism has been studied using ESR.

Results and Discussion

Design of Ligands and Synthesis of Complexes. Pyridyl groups are widely used for constructing extended structures by means of metal coordination. We have prepared bidentate 1,2-bis(2-methyl-5-(4-pyridyl)-3-thienyl)perfluorocyclopentene (**1a**) and monodentate 1-(2-methyl-5-phenyl-3-thienyl)-2-(2-methyl-5-(4-pyridyl)-3-thienyl)perfluorocyclopentene (**2a**) photochromic ligands by incorporating one or two pyridyl groups to the diarylethene backbone (Scheme 1). Phenyl derivative of this diarylethene, 1,2-bis(2-methyl-5-phenyl-3-thienyl)perfluorocyclopentene, has been reported to show photochromism in the crystalline phase. Zinc, copper, or manganese hexafluoroacetylacetonate was chosen for the metal source because of its high affinity for pyridyl ligands. Zn^{2+} complexes have no absorption in the visible region because of fully occupied d^{10} electronic structure. On the other hand, Cu^{2+} and Mn^{2+} complexes have unpaired electrons and show pale green and pale yellow colors, respectively.

Scheme 1

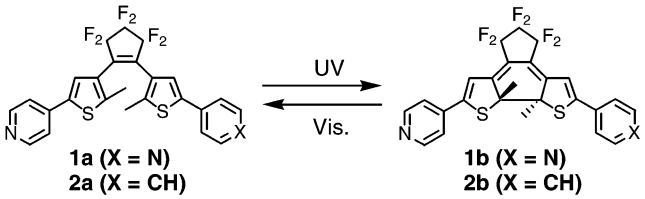

The colorless ethyl acetate solutions of **1a** or **2a** turned blue upon irradiation with UV light, indicating the formation of the closed-ring isomer **1b** or **2b**. The absorption maxima of closed-ring isomers **1b** and **2b** in ethyl acetate were 589 and 586 nm, respectively. The conversion from the open-ring to the closed-ring isomers under irradiation with 313 nm light was 98% for **1a**. The conversion of **2a** under irradiation with 333 nm light was 95%. The high conversion ratios are ascribable to low cycloreversion quantum yields.[13]

The complexation with transition metals was carried out by mixing dehydrated $M(hfac)_2$ (M = Zn, Cu, Mn) and diarylethene pyridyl ligand **1a** or **2a**. Successive recrystallization from appropriate solvents (see Experimental Section) gave **1a·Zn(hfac)$_2$**, **1a·Mn(hfac)$_2$**, **1a·Cu(hfac)$_2$**, **2a$_2$·Cu(hfac)$_2$**, **2a$_2$·Cu(hfac)$_2$·(hexane)**, and **2a$_2$·Zn(hfac)$_2$·(hexane)**. The colors of the complex crystals were colorless, yellow, and pale green for Zn, Mn, and Cu complexes, respectively. IR spectra of the crystal powders showed superposition of ligands and $M(hfac)_2$, indicating the formation of the complex. NMR spectra for zinc compounds and ESR spectra for manganese and copper compounds were consistent with the structures. Confirmation of the structure was finally performed by elemental analysis and X-ray crystallography.

Crystal Structure. The structures of the complexes were determined by X-ray crystallographic analysis. The complexes of bidentate ligand **1a** were chainlike structures. The crystal structures of the repeating unit were shown in Figure 1, and the chain structures were shown in Figure 2. The crystallographic parameters are summarized in Table 1. Two pyridyl nitrogens of two different molecules are coordinated with $M(hfac)_2$ in a *trans* configuration to form linear coordination polymers. All diarylethenes in the complex

(7) (a) Matsuda, K.; Irie, M. *Chem. Lett.* **2000**, 16−17. (b) Matsuda, K.; Irie, M. *J. Am. Chem. Soc.* **2000**, *122*, 7195−7201. (c) Matsuda, K.; Irie, M. *J. Am. Chem. Soc.* **2000**, *122*, 8309−8310. (d) Matsuda, K.; Matsuo, M.; Irie, M. *Chem. Lett.* **2001**, 436−437. (e) Matsuda, K.; Irie, M. *Chem. Eur. J.* **2001**, *7*, 3466−3473. (f) Matsuda, K.; Irie, M. *J. Am. Chem. Soc.* **2001**, *123*, 9896−9897. (g) Matsuda, K.; Matsuo, M.; Irie, M. *J. Org. Chem.* **2001**, *66*, 8799−8803. (h) Matsuda, K.; Matsuo, M.; Mizoguti, S.; Higashiguchi, K.; Irie, M. *J. Phys. Chem. B* **2002**, *106*, 11218−11225.

(8) (a) Leininger, S.; Olenyuk, B.; Stang, P. J. *Chem. Rev.* **2000**, *100*, 853−908. (b) Fujita, M.; Umemoto, K.; Yoshizawa, M.; Fujita, N.; Kusukawa, T.; Biradha, K. *J. Chem. Soc., Chem. Commun.* **2001**, 509−518.

(9) (a) Kahn, O. *Molecular Magnetism*; VCH: Weinheim, 1993. (b) Gatteschi, D. *Curr. Opin. Solid State Mater.* **1996**, *1*, 192. (c) Sano, Y.; Tanaka, M.; Koga, N.; Matsuda, K.; Iwamura, H.; Rabu, P.; Drillon, M. *J. Am. Chem. Soc.* **1997**, *119*, 8246−8252.

(10) (a) Kitaura, R.; Kitagawa, S.; Kubota, Y.; Kobayashi, T. C.; Kindo, K.; Mita, Y.; Matsuo, A.; Kobayashi, M.; Chang, H.-C.; Ozawa, T. C.; Suzuki, M.; Sakata, M.; Takata, M. *Science* **2002**, *298*, 2358−2361. (b) Eddaoudi, M.; Moler, D. B.; Li, H.; Chen, B.; Reineke, T. M.; O'Keeffe, M.; Yaghi, O. M. *Acc. Chem. Res.* **2001**, *34*, 319−330.

(11) (a) Munakata, M.; Wu, L. P.; Kuroda-Sowa, T.; Maekawa, M.; Suenaga Y.; Furuichi, K. *J. Am. Chem. Soc.* **1996**, *118*, 3305−3306. (b) Fernández-Acebes, A.; Lehn, J.-M. *Chem. Eur. J.* **1999**, *5*, 3285−3292. (c) Collins, G. E.; Choi, L.-S.; Ewing, K. J.; Michelet, V.; Bowen, C. M.; Winkler, J. D. *J. Chem. Soc., Chem. Commun.* **1999**, 321. (d) Fraysse, S.; Coudret, C.; Launay, J.-P. *Eur. J. Inorg. Chem.* **2000**, 1581−1590. (e) Murguly, E.; Norsten, T. B.; Branda, N. R. *Angew. Chem., Int. Ed.* **2001**, *40*, 1752−1755. (f) Konaka, H.; Wu, L. P.; Munakata, M.; Kuroda-Sowa, T.; Maekawa, M.; Suenaga, Y. *Inorg. Chem.* **2003**, *42*, 1928−1934.

(12) Preliminary communication has been reported. Matsuda, K.; Takayama, K.; Irie, M. *J. Chem. Soc., Chem. Commun.* **2001**, 363−364.

(13) (a) Irie, M.; Sakemura, K.; Okinaka, M.; Uchida, K. *J. Org. Chem.* **1995**, *60*, 8305−8309. (b) Matsuda, K.; Irie, M. *Tetrahedron Lett.* **2000**, *41*, 2577−2580.

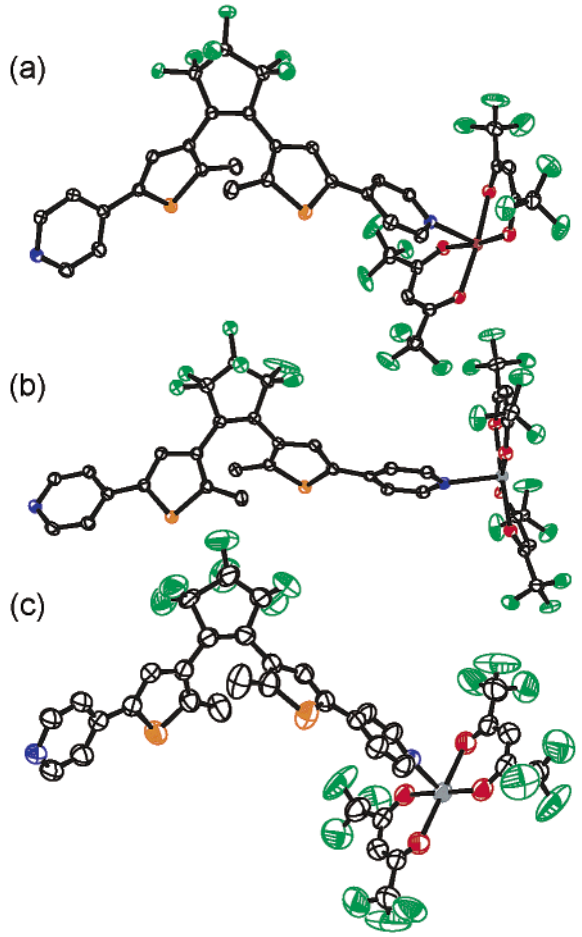

Figure 1. ORTEP drawings of the linear chain complexes of the open-ring isomer **1a** (50% probability): (a) **1a·Zn(hfac)$_2$**, (b) **1a·Mn(hfac)$_2$**, and (c) **1a·Cu(hfac)$_2$**. Hydrogen atoms are omitted for clarity. Only one repeating unit is shown.

Table 1. Crystallographic Parameters of Metal Complexes of the Open-Ring Isomer **1a**

	1a·Zn(hfac)$_2$[a]	**1a·Mn(hfac)$_2$**	**1a·Cu(hfac)$_2$**
formula	$C_{35}H_{18}F_{18}N_2O_4S_2Zn$	$C_{35}H_{18}F_{18}N_2O_4S_2Mn$	$C_{35}H_{18}F_{18}N_2O_4S_2Cu$
fw	1002.01	991.57	1000.17
T/K	111	95	293
cryst syst	monoclinic	triclinic	monoclinic
space group	$P2_1/c$	$P\bar{1}$	$P2/n$
a/Å	12.3592(9)	10.0408(7)	11.436(4)
b/Å	18.3531(14)	11.6439(8)	10.719(3)
c/Å	17.9411(13)	17.7049(13)	17.046(5)
α/deg		90.0680(10)	
β/deg	109.4780(10)	92.0120(10)	104.726(5)
γ/deg		112.1240(10)	
V/Å^3	3836.7(5)	1916.1(2)	2021.0(11)
Z	4	2	2
data/restraints/params	8418/0/561	9169/0/556	4440/0/352
*R*1 ($I > 2\sigma$)	0.0309	0.0409	0.0435
*wR*2 (all data)	0.0777	0.1042	0.1338

[a] Taken from ref 9.

adopted antiparallel conformation, in which photocyclization reactions take place by a conrotatory fashion.

The chain structure was dependent on the central metal ions. While the chain was zigzag shaped in the case of **1a·Zn(hfac)$_2$** and **1a·Cu(hfac)$_2$**, an almost straight chain was obtained in the case of **1a·Mn(hfac)$_2$**. The distances between the reactive carbons were 3.56, 3.58, and 3.77 Å for **1a·Zn(hfac)$_2$**, **1a·Mn(hfac)$_2$**, and **1a·Cu(hfac)$_2$**, respectively, which are short enough to react in the single-crystalline phase.[3i]

Table 2. Crystallographic Parameters of Metal Complexes of the Open-Ring Isomer **2a**

	2a$_2$·Cu(hfac)$_2$	**2a$_2$·Cu(hfac)$_2$·(hexane)**[a]	**2a$_2$·Zn(hfac)$_2$·(hexane)**[a]
formula	$C_{62}H_{36}F_{24}N_2O_4S_4Cu$	$C_{62}H_{36}F_{24}N_2O_4S_4Cu$	$C_{62}H_{36}F_{24}N_2O_4S_4Zn$
fw	1520.71	1520.71	1522.54
T/K	111	136	293
cryst syst	triclinic	monoclinic	monoclinic
space group	$P\bar{1}$	$C2/c$	$C2/c$
a/Å	8.900(2)	27.547(4)	27.867(6)
b/Å	10.774(3)	17.256(3)	17.212(4)
c/Å	17.648(5)	14.021(2)	13.922(3)
α/deg	86.483(4)		
β/deg	75.633(4)	90.181(3)	90.732(4)
γ/deg	72.277(4)		
V/Å^3	1561.4(7)	6664.8(17)	6677(2)
Z	2	4	4
data/restraints/params	6308/32/507	7160/0/438	6976/0/438
*R*1 ($I > 2\sigma$)	0.0476	0.0626	0.0787
*wR*2 (all data)	0.1384	0.1397	0.1865

[a] Hexane molecule incorporated in the crystal was eliminated by the SQUEEZE method.

A discrete 2:1 complex was formed from monodentate ligand **2a**. Figure 3 shows the discrete structures of **2a$_2$·Cu(hfac)$_2$**, **2a$_2$·Cu(hfac)$_2$·(hexane)**, and **2a$_2$·Zn(hfac)$_2$·(hexane)**. Crystallographic parameters were summarized in Table 2. For **2a$_2$·Cu(hfac)$_2$·(hexane)** and **2a$_2$·Zn(hfac)$_2$·(hexane)**, *n*-hexane molecule contained in the lattice were severely disordered and could not be resolved. The program SQUEEZE[14] in PLATON[15] was used to remove the *n*-hexane solvent density. The SQUEEZE method found a total electron count of 141 and 175 e in a volume of 807 and 840 Å^3 in the solvent regions of the unit cell for **2a$_2$·Cu(hfac)$_2$·(hexane)** and **2a$_2$·Zn(hfac)$_2$·(hexane)**, respectively. The calculated electron count for four hexanes is 200, which is substantially larger than observed. The elemental analysis data of vacuum-dried powdered crystals revealed 20% of hexane occupancy. These results suggest that the hexane molecules incorporated in the crystal lattice can easily evaporate. For three 1:2 complexes, **2a$_2$·Cu(hfac)$_2$**, **2a$_2$·Cu(hfac)$_2$·(hexane)**, and **2a$_2$·Zn(hfac)$_2$·(hexane)**, the distances between reactive carbons were 3.59, 3.53, and 3.53 Å, respectively, suggesting the photocyclization in the crystal lattice is possible. The **2a$_2$·Cu(hfac)$_2$·(hexane)** crystal and **2a$_2$·Zn(hfac)$_2$·(hexane)** crystal were isostructural except the metal center. Therefore, they were ideal for studying the effect of the different metal ions on the physical properties of the complexes.

The complexation of Cu(hfac)$_2$ and the isolated closed-ring isomers **1b** and **2b** afforded **1b$_2$·{Cu(hfac)$_2$}$_3$** and **2b$_2$·Cu(hfac)$_2$**. Crystallographic parameters were summarized in Table 3, and the molecular structures of **1b$_2$·{Cu(hfac)$_2$}$_3$** and **2b$_2$·Cu(hfac)$_2$** are shown in Figure 4. Closed-ring isomer **1b**, though this is a bidentate ligand, gave a discrete 2:3 complex. This may be attributed to the reduced coordination ability of the pyridyl ligand upon photocyclization.

(14) Van der Sluis, P.; Spek, A. L. *Acta Crystallogr., Sect. A* **1990**, *46*, 194−201.
(15) Spek, A. L. *Acta Crystallogra., Sect. A* **1990**, *46*, C34.

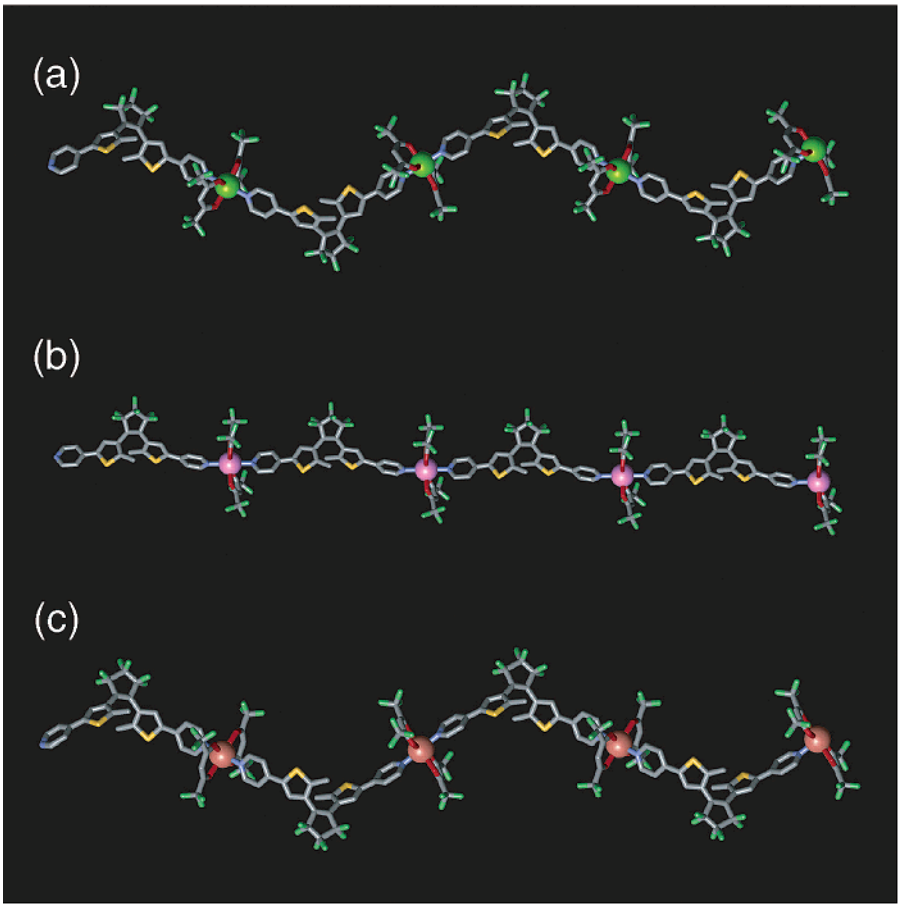

Figure 2. Linear chain structures of coordination polymers (a) **1a·Zn(hfac)$_2$**, (b) **1a·Mn(hfac)$_2$**, and (c) **1a·Cu(hfac)$_2$**.

Table 3. Crystallographic Parameters of Metal Complexes of the Closed-Ring Isomers **1b** and **2b**

	1b$_2$·{Cu(hfac)$_2$}$_3$	**2b$_2$·Cu(hfac)$_2$**
formula	$C_{80}H_{38}F_{48}N_4O_{12}S_4Cu_3$	$C_{62}H_{36}F_{24}N_2O_4S_4Cu$
fw	2478.02	1520.71
T/K	283	293
cryst syst	monoclinic	monoclinic
space group	$P2_1/c$	$P2_1/c$
a/Å	10.546(6)	9.796(3)
b/Å	20.176(10)	12.692(3)
c/Å	23.434(13)	24.549(6)
α/deg		
β/deg	91.76(2)	90.605(5)
γ/deg		
V/Å^3	4984(5)	3051.8(13)
Z	2	2
data/restraints/params	9638/0/703	6533/0/441
*R*1 ($I > 2\sigma$)	0.0616	0.0510
*wR*2 (all data)	0.1803	0.1353

In copper complexes, Cu^{2+} ions adopted an elongated tetragonal octahedral structure.[16] The bond lengths around copper atoms of the copper complexes are listed in Table 4. For all Cu complexes two of the axial Cu−O bonds in *trans* configuration were appreciably longer than four other equatorial bonds due to the Jahn−Teller distortion (Chart 1). The structures of the open-ring isomer and the closed-ring isomer were noticeably different for both bidentate and monodentate complexes. In the case of the bidentate ligand,

(16) Hathaway, B. J.; Billing, D. E. *Coord. Chem. Rev.* **1970**, *5*, 143−207.

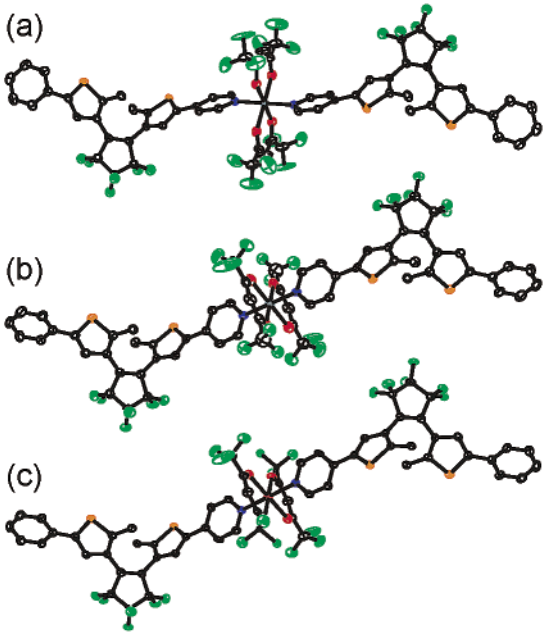

Figure 3. ORTEP drawings of X-ray crystallographic structures of discrete complexes of the open-ring isomer **2a** (50% probability): (a) **2a$_2$·Cu(hfac)$_2$**, (b) **2a$_2$·Cu(hfac)$_2$·(hexane)**, and (c) **2a$_2$·Zn(hfac)$_2$·(hexane)**. Hydrogen atoms are omitted for clarity.

the open-ring isomer complex **1a·Cu(hfac)$_2$** had the longer axial bond than closed-ring isomer complex **1b$_2$·{Cu(hfac)$_2$}$_3$**. As for the monodentate ligand, the closed-ring isomer complex **2b$_2$·Cu(hfac)$_2$** had the longer axial bond

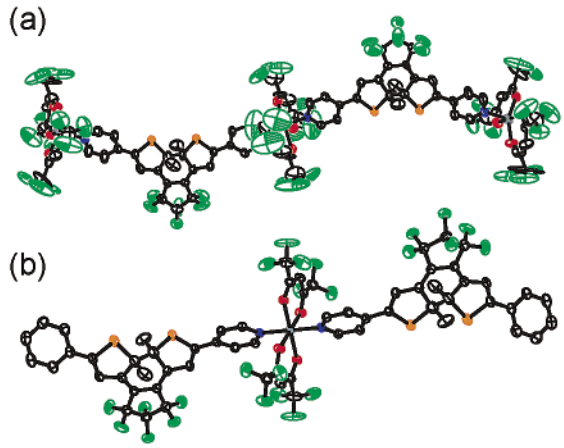

Figure 4. ORTEP drawings of X-ray crystallographic structures of discrete complexes of the closed-ring isomer **1b** and **2b** (50% probability): (a) **1b**$_2$·{**Cu(hfac)**$_2$}$_3$ and (b) **2b**$_2$·**Cu(hfac)**$_2$. Hydrogen atoms are omitted for clarity.

Table 4. Bond Lengths (Å) around Metal Centers in Cu Complexes

	1a·Cu-(hfac)$_2$	**1b$_2$·{Cu-(hfac)$_2$}$_3$**[a]	**2a$_2$·Cu-(hfac)$_2$**	**2b$_2$·Cu-(hfac)$_2$**
Cu−N	2.007(2)	1.995(7)	2.018(2)	2.008(3)
Cu−O(equatorial)	2.000(2)	2.022(7)	2.086(2)	1.999(2)
Cu−O(axial)	2.274(2)	2.194(8)	2.162(2)	2.288(3)

[a] Geometries around the central copper atoms.

Chart 1

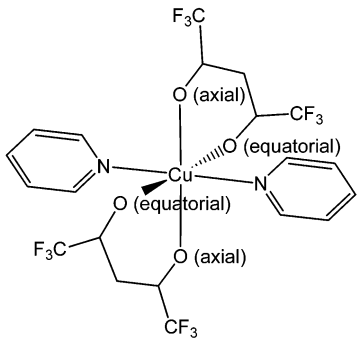

than open-ring isomer complex **2a$_2$·Cu(hfac)$_2$**. This difference is ascribed to the change in diarylethene pyridyl ligand, because the hexafluoroacetylacetone is the same. The difference will be discussed along with the ESR spectra.

Photochromic Reactions in Solution and in the Single-Crystalline Phase. The ethyl acetate solutions of the complexes underwent photochromic reactions by alternate irradiation with 313 and 578 nm light. The original solutions of the open-ring isomer complexes were slightly colored yellow for Mn complexes and green for Cu complexes due to the d−d transition of the metal ions. Upon irradiation with UV light, the solutions turned strongly blue. The blue color is due to the closed-ring isomers of diarylethenes. The absorption maxima of the colored isomers **1b·Zn(hfac)$_2$**, **1b·Mn(hfac)$_2$**, **1b·Cu(hfac)$_2$** were 590, 588, and 589 nm, respectively, which are the same as the maxima of **1b** itself in ethyl acetate solution (Figure 5).

The complex crystals also showed photochromic reactivity. Upon irradiation with 313 nm light the single crystals turned blue. Upon irradiation with 578 nm light the blue color disappeared. The complexation with metal ions did not

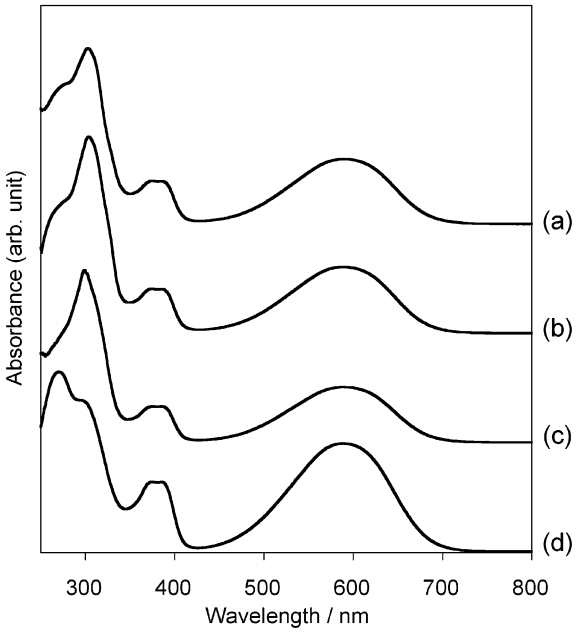

Figure 5. Absorption spectra of diarylethene complex after irradiation with 313 nm light in ethyl acetate: (a) **1a·Cu(hfac)$_2$**; (b) **1a·Mn(hfac)$_2$**; (c) **1a·Zn(hfac)$_2$**; and (d) **1a**.

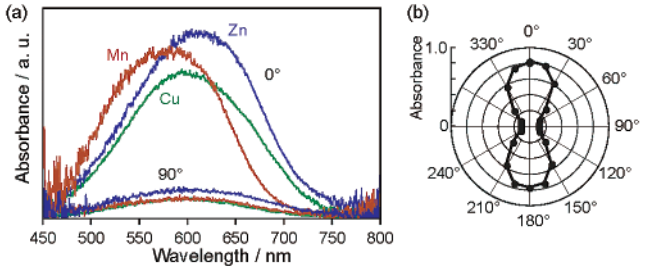

Figure 6. (a) Polarized absorption spectra of **1a·Zn(hfac)$_2$** (blue line), **1a·Mn(hfac)$_2$** (orange line), and **1a·Cu(hfac)$_2$** (green line) single crystals. For manganese and copper complexes, the direction of the maximum intensity was defined as 0°. For zinc complex, [20$\bar{1}$] direction, the direction of the linear polymer chain was defined as 0°. (b) Polar plot of polarized absorption of **1a·Zn(hfac)$_2$** measured at 620 nm.

prohibit the photochromic reactions of the diarylethene units in the single-crystalline phase.

The color of the crystals was observed under polarized light. Figure 6 shows the polarized absorption spectra of **1a·Zn(hfac)$_2$**, **1a·Mn(hfac)$_2$**, and **1a·Cu(hfac)$_2$** crystals and the polar plot of the **1a·Zn(hfac)$_2$** crystal. Upon rotation, the absorption maxima did not change, but the intensities dramatically changed. The blue color intensity changes by rotating the crystals, indicating that the closed-ring isomers are regularly oriented in the crystals. In other words, the photochromic reactions proceed in the crystal lattice. The absorption maxima were 620, 580, and 600 nm for **1a·Zn(hfac)$_2$**, **1a·Mn(hfac)$_2$**, and **1a·Cu(hfac)$_2$** crystals, respectively. The absorption maxima in crystals were different among the complexes, while they are similar in solutions.

The relation between the transition moment and the crystal structure was examined on the face-indexed crystal of **1a·Zn(hfac)$_2$**. The polar plot measured normal to (010) plane is shown in Figure 6b. In this plot, [20$\bar{1}$] direction, the direction of the linear polymer chain is defined as 0°. The

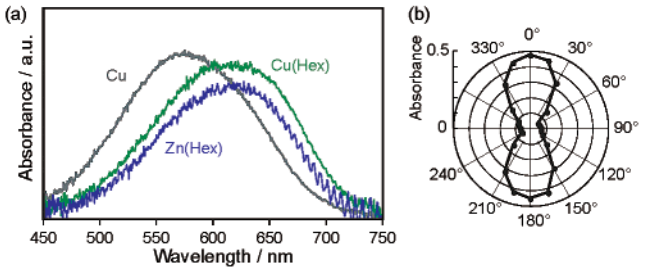

Figure 7. (a) Polarized absorption spectra of single crystal of **2a$_2$·Cu(hfac)$_2$** (gray line), **2a$_2$·Cu(hfac)$_2$·(hexane)** (green line), **2a$_2$·Zn(hfac)$_2$·(hexane)** (blue line). The direction of the maximum intensity was defined as 0°. (b) Polar plot of polarized absorption of **2a$_2$·Cu(hfac)$_2$** measured at 580 nm.

maximum of the absorption was identical to the direction of the linear polymer chain.

Monodentate complexes also showed photochromic reactivity in the single-crystalline phase. Figure 7 shows the polarized absorption spectra of **2a$_2$·Cu(hfac)$_2$**, **2a$_2$·Cu(hfac)$_2$·(hexane)**, and **2a$_2$·Zn(hfac)$_2$·(hexane)** crystals and the polar plot of the **2a$_2$·Cu(hfac)$_2$** crystal. The absorption maximum of **2a$_2$·Cu(hfac)$_2$** was observed at 580 nm, while the absorption maxima of **2a$_2$·Cu(hfac)$_2$·(hexane)** and **2a$_2$·Zn(hfac)$_2$·(hexane)** were observed at 620 nm. As mentioned in the crystallography section, **2a$_2$·Cu(hfac)$_2$·(hexane)** and **2a$_2$·Zn(hfac)$_2$·(hexane)** were isostructural. The isostructural crystals **2a$_2$·Cu(hfac)$_2$·(hexane)** and **2a$_2$·Zn(hfac)$_2$·(hexane)** showed the same absorption maxima regardless of the difference in the metal ions, while absorption maximum of **2a$_2$·Cu(hfac)$_2$** showed hypsochromic shift. This strongly suggests that the absorption spectrum of the closed-ring isomers is determined by the conformation of the diarylethene units, not by the metal ions. The absorption spectra of the closed-ring forms of diarylethenes are dependent on the torsion angle between the thiophene ring and the terminal phenyl or pyridyl ring.[17]

ESR Study. X-band ESR spectra of copper complexes were measured in a toluene matrix at 60−70 K for **1a·Cu(hfac)$_2$** and **2a$_2$·Cu(hfac)$_2$** (Figure 8). The complex of open-ring ligand **1a** (Figure 8a, black) showed a typical axial-type Cu^{2+} spectrum in which g_x and g_y are almost the same. The simulation of the spectrum gave $g_\perp = 2.08$, $g_\parallel = 2.34$, and $A_\parallel = 160$ G.[18] The values suggest the elongated tetragonal octahedral structure in which two coordination bonds in *trans* configuration are longer than the others as determined in X-ray crystallographic analysis. Upon irradiation with UV light, the spectrum changed along with the photochromism. The irradiation was performed in solution and in the frozen matrix. In both cases, the spectral change was observed. After irradiation with visible light, the original spectrum was regenerated. The conversion from the open-ring to the closed-ring isomers in the photostationary state was estimated to be more than 90%. The spectrum of the photogenerated closed-ring isomer could be reproduced by

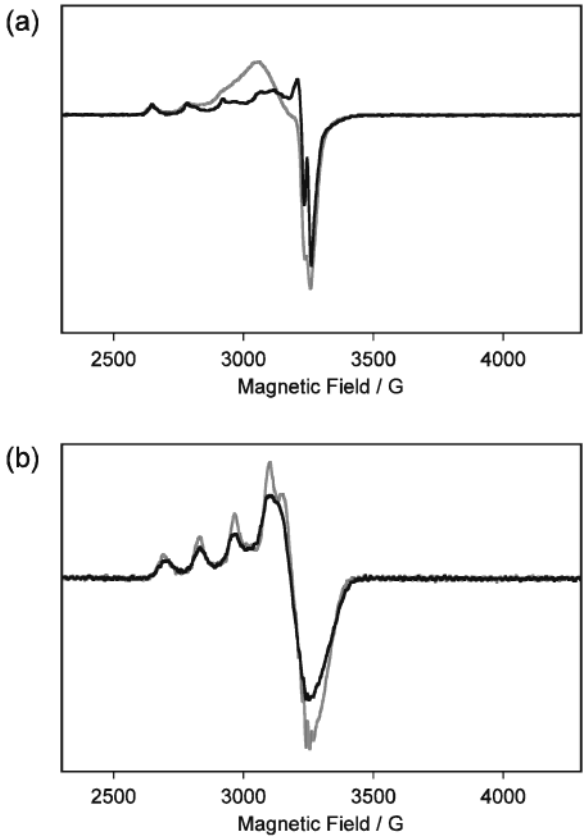

Figure 8. (a) X-band ESR spectra of **1a·Cu(hfac)$_2$** in toluene matrix (1 mM) measured at 70 K (9.36 GHz). (b) X-band ESR spectra of **2a$_2$·Cu(hfac)$_2$** in toluene matrix (1 mM) measured at 60 K (9.36 GHz). Measurement was performed before (black) and after (gray) irradiation with UV light. Irradiation with visible light reproduced the original spectra.

using three different g values, $g_1 = 2.07$, $g_2 = 2.17$, and $g_3 = 2.34$ (Figure 8a, red). This is a typical rhombic spectrum, which is observed in elongated rhombic octahedral stereochemistry.[16] The photoisomerization reaction of the diarylethene unit caused the distortion in the copper center.

In the case of **2a$_2$·Cu(hfac)$_2$**, the spectral change before and after irradiation of UV light was not so significant (Figure 8b). Both the open-ring isomer and the closed-ring isomer had axial-type spectra, with $g_\perp = 2.08$, $g_\parallel = 2.31$, and $A_\parallel = 150$ G.

These results of the ESR measurement suggest that the coordination structures around Cu^{2+} ion changed from elongated tetragonal octahedral in **1a** to elongated rhombic octahedral in **1b**, while the structures of the complexes of **2a** and **2b** were similar each other. Because the exchange coupling between two Cu^{2+} ions through more than 17 Å of distance is negligibly small, the difference should originate from the difference in the ligands.

Some possibilities for the origin of this spectral change are taken into consideration. Since the hexafluoroacetylacetone ligand is the same, the difference between open-ring and closed-ring isomers of the diarylethene pyridyl ligand had induced spectral change. As shown in the X-ray crystallography section, geometry around Cu^{2+} ion changed along with photochromism. The shortening of the bond length of the axial ligand in **1** upon photocyclization was

(17) Morimoto, M.; Kobatake, S.; Irie, M. *Chem. Eur. J.* **2003**, *9*, 621−627.

(18) Simulation was performed using *EPRSim XOP* program by John Boswell, Oregon Graduate Institute, an adaptation of *QPOW* program by Mark J. Nilges and R. Linn Belford.

observed in molecular structure. This means the relative increase of the axial ligand field of the Cu^{2+} ion, namely the relative decrease of the equatorial ligand field of the diarylethene pyridyl ligand.[19] This decrease of the equatorial ligand field can be ascribed to the decrease in the π-acceptor character of the ligand along with photocyclization. The change in the photochromic ligand may induce the coordination structure and the ESR spectrum. In the case of the X-ray structure of **2**, the bond length of the axial ligand got even longer, so that the ESR spectrum did not change.

We have also reported that diarylethenes shrink along with photocyclization.[20] The shrinkage in size in **1** cannot be relieved by the movement of the diarylethene molecules because both ends of the molecule are coordinating to different metal ions. The shrinkage of the diarylethene units is accumulated in the coordination polymer, the coordination structure is distorted, and the ESR spectra are changed significantly. On the contrary, as **2** is monodentate, the complex is composed of two diarylethene molecules and one metal ion, so that the ESR spectra changed only slightly.

Both possibilities suggest that the ESR spectral change is due to the distortion around the Cu^{2+} center upon photoisomerization. Photoinduced structural change in the organic ligand caused the structural change in the metal complex.

Conclusions

We have synthesized metal complexes composed of bidentate and monodentate diarylethene pyridyl ligands and transition metal ions. The complexes underwent reversible photochromic reactions in the single-crystalline phase as well as in solution. The complexation with metal ions does not prohibit the photochromic reactions in the single-crystalline phase. The ESR spectra of the copper complexes of **1a** in toluene matrices at 70 K were reversibly interconverted by irradiation with UV and visible light. It was concluded that photochromic reaction of the ligand caused the change of the coordination structure.

Experimental Section

(A) Materials. ^{1}H NMR spectra were recorded on Varian Gemini 200 and JEOL JNM-ECP400 instruments. UV−vis spectra were recorded on a Hitachi U-3500 spectrophotometer. Mass spectra were obtained by a Shimadzu QP-5050A spectrometer. Zn(II), Mn(II), and Cu(II) hexafluoroacetylacetonates were purchased from TCI. Melting points are not corrected. Compound **1a** was synthesized according to the literature.[6b]

1-(2-Methyl-5-phenyl-3-thienyl)-2-(2-methyl-5-(4-pyridyl)-3-thienyl)-3,3,4,4,5,5-hexafluorocyclopentene (2a). To a well stirred solution of 2-methyl-3-bromo-5-(4-pyridyl)-thiophene (2.2 g, 8.5 mmol) in anhydrous THF (100 mL) under Ar at −78 °C was added dropwise 1.6 M *n*-BuLi in hexane (5.6 mL, 9.0 mmol), and stirring was continued for 2 h at −78 °C. Then, a solution of 3-(2,3,3,4,4,5,5-heptafluorocyclopent-1-en-1-yl)-2-methyl-5-phenylthiophene (3.3 g, 9.0 mmol) was added dropwise. The mixture was stirred for 4 h and allowed to warm to room temperature, and aqueous NH_4Cl was added. The resultant mixture was then extracted with Et_2O, and the organic extract was washed with brine and dried ($MgSO_4$). The solvent was removed. Column chromatography (silica gel, CH_2Cl_2/AcOEt = 4:1) afforded dithienylethene **2a** (3.6 g, 81%) as a slightly green powder: mp 154.5−155.0 °C; ^{1}H NMR (200 MHz, $CDCl_3$) δ 1.96 (s, 3 H), 2.00 (s, 3 H), 7.2−7.6 (m, 9 H), 8.60 (d, J = 6.2 Hz, 2 H); ^{13}C NMR (100 MHz, $CDCl_3$) δ 14.6, 14.7, 119.5, 122.3, 124.9, 125.6, 126.4, 128.0, 129.1, 133.2, 139.1, 140.3, 141.3, 142.6, 143.7, 150.6; ^{19}F NMR (376 MHz, $CDCl_3$, CF_3COOH as external reference) δ −132.4, −110.5, −110.7; MS m/z 521 ($[M]^+$), 506 ($[M - CH_3]^+$), 491($[M - 2CH_3]^+$); UV−vis (AcOEt) λ_{max} 285 nm; after irradiation with 313 nm light (AcOEt) λ_{max} 308, 586 nm; Anal. Calcd for $C_{26}H_{17}F_6NS_2$: C, 59.88; H, 3.29; N, 2.69. Found: C, 60.03; H, 3.41; N, 2.68.

1a·Zn(hfac)$_2$. To a solution of **1a** (50 mg, 96 μmol) in dichloromethane (2 mL) was added a solution of $Zn(hfac)_2 \cdot 2H_2O$ (49 mg, 95 μmol) in dichloromethane/methanol (1:1, v/v) (2 mL). Pale green precipitates were collected and recrystallized from dichloromethane/methanol (1:1, v/v) to afford colorless block crystals: mp 274 °C (decomp); ^{1}H NMR (400 MHz, DMSO-d_6) δ 2.01 (s, 6 H), 5.55 (s, 2 H), 7.65 (d, J = 3.5 Hz, 4 H), 7.83 (s, 2 H), 8.59 (brs, 4 H); IR (KBr) ν 1130, 1250, 1500, 1600 cm^{-1}; UV−vis (AcOEt) λ_{max} 300 nm; after irradiation with 313 nm light (AcOEt) λ_{max} 590 nm; Anal. Calcd for $C_{35}H_{18}F_{18}N_2O_4S_2Zn$: C, 41.95; H, 1.81; N, 2.80. Found: C, 42.13; H, 1.82; N, 2.95.

1a·Mn(hfac)$_2$. To a solution of **1a** (200 mg, 380 μmol) in dichloromethane (2 mL) was added a solution of $Mn(hfac)_2 \cdot xH_2O$ (179 mg) in dichloromethane/methanol (1:1, v/v) (2 mL). After solvents are evaporated, precipitates were recrystallized from dichloromethane/methanol (1:1, v/v) to afford yellow block crystals: mp >200 °C (decomp); IR (KBr) ν 1130, 1240, 1480, 1600 cm^{-1}; UV−vis (AcOEt) λ_{max} 301 nm; after irradiation with 313 nm light (AcOEt) λ_{max} 588 nm. Anal. Calcd for $C_{35}H_{18}F_{18}N_2O_4S_2Mn$: C, 42.40; H, 1.83; N, 2.83. Found: C, 42.40; H, 1.83; N, 2.77.

1a·Cu(hfac)$_2$. To a solution of **1a** (200 mg, 380 μmol) in dichloromethane (2 mL) was added a solution of $Cu(hfac)_2 \cdot xH_2O$ (182 mg) in dichloromethane/methanol (1:1, v/v) (2 mL). Precipitates were collected and recrystallized from THF/methanol (1:1, v/v) to afford pale green block crystals: mp >200 °C (decomp); IR (KBr) ν 1130, 1250, 1500, 1610 cm^{-1}; UV−vis (AcOEt) λ_{max} 300 nm; after irradiation with 313 nm light (AcOEt) λ_{max} 589 nm. Anal. Calcd for $C_{35}H_{18}F_{18}N_2O_4S_2Cu$: C, 42.03; H, 1.81; N, 2.80. Found: C, 41.89; H, 1.82; N, 2.90.

2a$_2$·Cu(hfac)$_2$. To a solution of **2a** (45 mg, 86 μmol) in toluene (1 mL) was added a solution of $Cu(hfac)_2 \cdot xH_2O$ (21 mg) in toluene (0.5 mL). Precipitates were collected and recrystallized from 2-propanol to afford pale green block crystals: mp 182.6−183.0 °C; UV−vis (AcOEt) λ_{max} 297 nm; after irradiation with 333 nm light (AcOEt) λ_{max} 589 nm. Anal. Calcd for $C_{62}H_{36}F_{24}N_2O_4S_4Cu$: C, 48.97; H, 2.39; N, 1.84. Found: C, 49.08; H, 2.40; N, 1.96.

2a$_2$·Cu(hfac)$_2$·(hexane). To a solution of **2a** (41 mg, 79 μmol) in dichloromethane was added $Cu(hfac)_2 \cdot xH_2O$ (19 mg) in dichloromethane. After the solvent was evaporated, the residue was recrystallized from dichloromethane/hexane (1:1, v/v) to give pale green block crystals. Anal. Calcd for $C_{62}H_{36}F_{24}N_2O_4S_4Cu \cdot (C_6H_{14})_{0.2}$: C, 49.36; H, 2.54, N, 1.82. Found: C, 49.32; H, 2.64; N, 2.09.

2a$_2$·Zn(hfac)$_2$·(hexane). To a solution of **2a** (22 mg, 42 μmol) in dichloromethane was added $Zn(hfac)_2 \cdot 2H_2O$ (10 mg, 19 μmol) in dichloromethane. After the solvent was evaporated, the residue was recrystallized from hexane to give colorless block crystals: ^{1}H NMR (200 MHz, $CDCl_3$) δ 1.94 (s, 6 H), 2.01 (s, 6 H), 5.97 (s, 2 H), 7.26−7.55 (m, 18 H), 8.57 (brs, 4 H). Anal. Calcd for

(19) Lever, B. P.; Mantovani, E. *Inorg. Chem.* **1971**, *10*, 817.
(20) Irie, M.; Kobatake, S.; Horichi, M. *Science*, **2001**, *291*, 1769−1772.

$C_{62}H_{36}F_{24}N_2O_4S_4Zn(C_6H_{14})_{0.2}$: C, 49.30; H, 2.54, N, 1.82. Found: C, 49.36; H, 2.79; N, 1.78.

(B) Photochemical Measurement. Solvents used for physical measurements were spectroscopic grade and purified by distillation before use. Absorption spectra were measured on a spectrophotometer (Hitachi U-3500). Absorption spectra in single-crystalline phases were measured by using a Leica DMLP polarizing microscope connected with Hamamatsu PMA-11 detector. The polarizer and analyzer were set parallel to each other.

Photoirradiation was carried out by using a USHIO 500 W super high-pressure mercury lamp and a USHIO 500-W xenon lamp. Mercury lines of 313, 333, 578 nm were isolated by passing the light through a combination of a Toshiba band-pass filter or a cutoff filter and a monochromator (Ritsu MC-20L).

(C) Crystallography. The data collection was performed on a Bruker SMART1000 CCD-based diffractometer (50 kV, 40 mA) with Mo Kα radiation. The data were collected as a series of ω-scan frames, each with a width of 0.3°/frame. The crystal-to-detector distance was 5.118 cm. Crystal decay was monitored by repeating the 50 initial frames at the end data collection and analyzing the duplicate reflections. Data reduction was performed using SAINT-PLUS software,[21] which corrects for Lorentz and polarization effects, and decay. The cell constants were calculated by the global refinement. The structure solved by direct methods and refined by full least-squares on F^2 using SHELXL software.[22] The positions of all hydrogen atoms were calculated geometrically and refined by the riding model. Several hexafluorocyclopentene ring had disorder originating from ring-flipping, and the disordered part was refined isotropically. For **2a$_2$·Cu(hfac)$_2$·(hexane)** and **2a$_2$·Zn(hfac)$_2$·(hexane)**, *n*-hexane molecule contained in the lattice were severely disordered and could not be resolved. The program SQUEEZE[14] in PLATON[15] was used to remove the *n*-hexane solvent density.

(D) ESR Spectroscopy. A Bruker ESP 300E spectrometer was used to obtain X-band ESR spectra. Temperatures were controlled by an RMC CT-470-ESR cryogenic temperature controller. The cryostat was maintained at high vacuum by a turbo molecular/rotary pump set. The sample was dissolved in solvent (ca. 1 mM) and degassed with argon bubbling for 5 min.

Acknowledgment. This work was partly supported by a Grant-in-Aid for the 21st Century COE Program, "Functional Innovation of Molecular Informatics", from the Ministry of Education, Culture, Sports, Science and Technology of Japan. The measurement of ^{13}C and ^{19}F NMR was made using JEOL JNM-ECP400 spectrometer at the Center of Advanced Instrumental Analysis, Kyushu University

Supporting Information Available: The photochromic reaction of **2a** in ethyl acetate and the result of X-ray crystallographic analysis of **2a**. X-ray crystallographic data of **1a·Mn(hfac)$_2$**, **1a·Cu(hfac)$_2$**, **2a$_2$·Cu(hfac)$_2$**, **2a$_2$·Cu(hfac)$_2$·(hexane)**, **2a$_2$·Zn(hfac)$_2$·(hexane)**, **1b$_2$·{Cu(hfac)$_2$}$_3$**, **2b$_2$·Cu(hfac)$_2$, and 2a** (CIF). This material is available free of charge via the Internet at http://pubs.acs.org.

IC035020R

(21) *SAINTPLUS Software Package*, Version 6; Bruker AXS: Madison, WI, 2001.

(22) *SHELXTL Software Package*, Version 5; Bruker AXS: Madison, WI, 2001.